

A simple bipartite graph projection model for clustering in networks

Austin R. Benson ^{*}, Paul Liu [†], and Hao Yin [‡]

Abstract. Graph datasets are frequently constructed by a projection of a bipartite graph, where two nodes are connected in the projection if they share a common neighbor in the bipartite graph; for example, a coauthorship graph is a projection of an author-publication bipartite graph. Analyzing the structure of the projected graph is common, but we do not have a good understanding of the consequences of the projection on such analyses. Here, we propose and analyze a random graph model to study what properties we can expect from the projection step. Our model is based on a Chung-Lu random graph for constructing the bipartite representation, which enables us to rigorously analyze the projected graph. We show that common network properties such as sparsity, heavy-tailed degree distributions, local clustering at nodes, the inverse relationship between node degree, and global transitivity can be explained and analyzed through this simple model. We also develop a fast sampling algorithm for our model, which we show is provably optimal for certain input distributions. Numerical simulations where model parameters come from real-world datasets show that much of the clustering behavior in some datasets can just be explained by the projection step.

1. Networks as bipartite projections. Networks or graphs that consist of a set of nodes and their pairwise interactions are pervasive models throughout the sciences. Oftentimes, network datasets are constructed by a “projection” of a bipartite graph [39, 43, 53, 64]; specifically, given a bipartite graph with left and right nodes, the *one-mode projection* is a (unipartite) graph on the left nodes, where two left nodes are connected if they share a common right node neighbor in the bipartite graph. In many cases, these projections are explicit in the data construction process, such as connecting diseases associated with the same gene [28], people belonging to the same group or team [45, 51], and ingredients appearing in common recipes [1, 54]. In other cases, the projection is more implicit. For example, the connections in a social network often arise due to shared interests [14]. Regardless, even though a bipartite graph is more expressive than its projection, analyzing the projection still leads to valuable data insights [56, 62], enables the use of standard network analysis tools [9, 37, 63], and can even be used to make predictions about the bipartite graph itself [8].

For network analysis, it is paramount to know if structural properties in the data arise from some phenomena of the system under study or are simply consequences of a mathematical property of the graph construction process. Random graph models can serve as null models for making such distinctions [25]. Often, the random graph model maintains some property of the network data (at least approximately or in expectation) and then direct mathematical analysis of the random graph can be used to determine whether certain structural properties will arise as a consequence. For example, Chung and Lu showed that short average path lengths can be a consequence of a uniform sample of a random graph with an expected power law degree distribution [18].

Here, we analyze a simple random graph model that explains some properties of projected

^{*}Department of Computer Science, Cornell University, Ithaca, NY, USA (arb@cs.cornell.edu).

[†]Department of Computer Science, Stanford University, Stanford, CA, USA (paul.liu@stanford.edu)

[‡]Institute for Computational and Mathematical Engineering, Stanford University, Stanford, CA, USA (yinh@stanford.edu)

graphs. More specifically, the random graph model is a projection of a bipartite “Chung-Lu style” model. Each left and right node in the bipartite graph has a weight, and the probability of an edge is proportional to the product of these weights.

The simplicity of this model enables theoretical analysis of properties of the projected graph. One fundamental property is *clustering*: even in a sparse network, there is a tendency of edges to appear in small clusters or cliques [24, 46, 57]. There are various explanations for clustering, including local evolutionary processes [31, 29, 52], hierarchical organization [47], and community structure [50]. Here, we show how clustering can arise just from bipartite projection. We derive an explicit equation for the expected value of a probabilistic variant of the *local clustering coefficient* of a node (the fraction of pairs of neighbors of the node that are connected) as a function of its weight in the model.

We show that local clustering decreases with the inverse of the weight, while expected degree grows linearly with the weight, which is consistent with prior empirical measurements [41, 50], mean-field analysis of models that explicitly incorporate clustering [52], and certain random intersection graph models [13]. Thus, the weights in the bipartite model are a potential confounding factor for this relationship between degree and clustering.

In addition, using weight distributions fit from real-world bipartite graph data, we show that high levels of clustering and clustering levels at a given degree are often just a consequence of bipartite projection. However, in several datasets, there is still a gap between the clustering levels in the data and in the model. Bipartite projection has been mentioned informally as a reason for clustering in several datasets [26, 42, 44], and a recent study has shown that sampling from *configuration models* of hypergraphs and projecting can also reproduce clustering [17]. Our analysis provides theoretical justifications and further explanations for these claims, and also shows that the global clustering (also called transitivity) tends towards a positive constant as the bipartite network grows large. We also analyze a recently introduced measure of clustering called the closure coefficient [60, 61] under our projection model and find that the expected local closure coefficient of every node is the same, which aligns with some prior empirical results [60].

In addition to clustering, we analyze several properties of the bipartite random graph and its projection. For instance, we show that if the weight distribution on the left and right nodes follow a power law, then the degree distribution for those nodes is also a power law in the bipartite graph; moreover, the degrees in the projected graph will also follow a power law. Thus, heavy-tailed degree distributions in the projected graph can simply be a consequence of a process that creates heavy-tailed degree distributions in the bipartite graph. Furthermore, we show that the projected graph is sparse in the sense that, under a mild restriction on the maximum weight, the probability of an edge between any two nodes goes to zero as the number of nodes in the projected graph grows to infinity. Combined with our results on clustering, our model thus provides a large class of networks that are “locally dense but globally sparse” [58].

1.1. Preliminaries. We consider networks as undirected graphs $G = (V, E)$ without self-loops and multi-edges. We use $d(u)$ to denote the degree of node u (the number of edges incident to node u) and $T(u)$ to denote the number of triangles (3-cliques) containing node u . A *wedge* is a pair of edges that shared a common node, and the common node is the *center* of the wedge. A statistic of primary interest is the *clustering coefficient*:

Definition 1.1. The local clustering coefficient of a node $u \in V$ is $\tilde{C}(u) = \frac{2T(u)}{d(u)(d(u)-1)}$, i.e., the chance that a randomly chosen wedge centered at u induces a triangle.

At the network level, the global clustering coefficient \tilde{C}_G is the probability that a randomly chosen wedge in the entire graph induces a triangle, i.e., $\tilde{C}_G = \frac{\sum_{u \in V} 2T(u)}{\sum_{u \in V} d(u)(d(u)-1)}$.

A closely related measure of clustering is the conditional probability of edge existence given the wedge structure [10, 13, 22]. Specifically, we have the following analogs of the local and global clustering coefficients:

$$(1.1) \quad C_G = \mathbb{P}[(v, w) \in E \mid (u, v), (u, w) \in E],$$

where all the nodes $u, v, w \in V$ are unspecified, while the local clustering coefficient is

$$(1.2) \quad C(u) = \mathbb{P}[(v, w) \in E \mid (u, v), (u, w) \in E],$$

where u is the specified node. In both cases, (u, v) and (u, w) comprise a random wedge from the graph. In this paper, we use these slightly different definitions of clustering based on conditional edge existence, as they are more amenable to analysis.

An alternative clustering metric is the recently proposed *closure coefficient* [60, 61].

Definition 1.2. The local closure coefficient of a node $u \in V$ is $\tilde{H}(u) = \frac{2T(u)}{W_h(u)}$, where $W_h(u)$ is the number of length-2 paths leaving vertex u . In other words, the closure coefficient is the chance that a randomly chosen 2-path emanating from u induces a triangle.

Analogously, the conditional probability variant of the closure coefficient is:

$$(1.3) \quad H(u) = \mathbb{P}[(u, w) \in E \mid (u, v), (v, w) \in E],$$

where u is the specified node.

The global closure coefficient is equal to the global clustering coefficient, as the number of 2-paths is exactly equal to the number of wedges. This is true for both the non-conditional and the conditional probability variant. In Appendix A, we show that the conditional probability definitions above correspond to a weighted average over the standard definitions of clustering and closure. Henceforth when referring to the clustering or closure coefficients, we always refer to the conditional probability variant.

Next, a graph is *bipartite* if the nodes can be partitioned into two disjoint subsets $L \sqcup R$, which we call the *left* and *right* nodes, and any edge is between one node from L and one node from R . We denote a bipartite graph by $G_b = (V_b, E_b)$ with $V_b = L \sqcup R$, and call L and R the left and right side of the bipartite graph. The number of nodes on each side is denoted by $n_L = |L|$ and $n_R = |R|$, and $n_b = |V_b| = n_L + n_R$ is the total number of nodes. Analogously, for any node $u \in V_b$, we use $d_b(u)$ as its degree.

The *projection* of a bipartite graph is the primary concept we analyze.

Definition 1.3. A projection of a bipartite graph $G_b = (L \sqcup R, E_b)$ is the graph $G = (L, E)$, where the nodes are the left nodes of the bipartite graph and the edges connect any two nodes in L that connect to some node $r \in R$ in the bipartite graph. More formally,

$$(1.4) \quad E = \{(u, v) \mid u, v \in L, u \neq v, \text{ and } \exists z \in R \text{ for which } (u, z), (v, z) \in E_b\}.$$

If there is more than one right node z that connects to left nodes u and v in the bipartite graph, the projection only creates a single edge between u and v .

Given a dataset, one can project onto the left or right nodes. One can always permute the left and right nodes, and we assume projection onto the left nodes L for notational consistency.

Several statistical properties of the models we consider will use samples drawn from a power law distributions, which are prevalent in network data models [21].

Definition 1.4. *The probability density function of the power law distribution, parametrized by $(\alpha, w_{\min}, w_{\max})$ with $\alpha > 1$ and $0 < w_{\min} < w_{\max} \leq \infty$, is*

$$f(w) = \begin{cases} Cw^{-\alpha} & \text{if } w \in [w_{\min}, w_{\max}] \\ 0 & \text{otherwise} \end{cases}$$

where $w > 0$ is any real number and $C = (w_{\min}^{1-\alpha} - w_{\max}^{1-\alpha})/(\alpha - 1)$ is a normalizing constant.

For a discrete power-law (or Zipfian) distribution, we restrict w to integer values inside $[w_{\min}, w_{\max}]$ and adjust the normalization constant accordingly.

The parameter α is the decay exponent of the distribution, while w_{\min} and w_{\max} specify range. For simplicity, we assume that $w_{\min} = 1$ and $w_{\max} = \Omega(1)$ throughout this paper.

When the maximum range is not specified, *i.e.*, $w_{\max} = \infty$, a standard result on the maximum statistics of power-law samples is the following:

Lemma 1.5 (Folklore). *For a discrete or continuous power-law distribution \mathcal{D} with parameters $(\alpha, w_{\min} = 1, w_{\max} = \infty)$ and *i.i.d.* samples $w_1, w_2, \dots, w_n \sim \mathcal{D}$, $\mathbb{E}[\max_i w_i] = n^{\frac{1}{\alpha-1}}$.*

2. Models for Bipartite Projection. In this section we formalize our model and give some background on relevant models for projection and graph generation. Our model is an extension of the seminal random graph model from Chung and Lu [18]. The classical Chung-Lu model takes as input a weight sequence S , which specifies a nonnegative weight w_u for each node, and then produces an undirected edge (u, v) with probability $w_u w_v / \sum_z w_z$. To make sure that the probabilities are well defined, the model assumes that $\max_u w_u^2 \leq \sum_v w_v$. Along similar lines, Aksoy et al. introduced a Chung-Lu-style bipartite random graph model based on realizable degree sequences [3]. In general, the model we use is quite similar. However, our focus in this paper is to analyse the effects of projection on such models.

2.1. Our Chung-Lu Style Bipartite Projection Model. Our model takes as input the number of left nodes n_L , the number of right nodes n_R , and two sequences of weights S_L and S_R for the left and right nodes. We denote the weight of any node u by w_u . The model then samples a random bipartite graph $G_b = (L \sqcup R, E_b)$, where

$$(2.1) \quad \mathbb{P}[(u, v) \in E_b \mid w_u, w_v] = \min\left(\frac{w_u w_v}{\sum_{z \in R} w_z}, 1\right), \quad u \in L, v \in R.$$

After generating the graph, we project the graph following Definition 1.3, which is itself a random graph. This model is similar to the inhomogeneous random intersection graph [12] (see subsection 2.3 for more details).

Our analysis will depend on properties of S_L and S_R and the moments of these sequences. We denote the k th-order moments of S_L and S_R by M_{Lk} and M_{Rk} for integers $k \geq 1$:

$$(2.2) \quad M_{Lk} = \frac{1}{n_L} \sum_{u \in L} w_u^k, \quad M_{Rk} = \frac{1}{n_R} \sum_{v \in R} w_v^k.$$

With this notation, we can re-write the edge probabilities as

$$(2.3) \quad \mathbb{P}[(u, v) \in E_b \mid w_u, w_v] = \min\left(\frac{w_u w_v}{n_R M_{R1}}, 1\right).$$

Remark 2.1. The model is invariant upon uniform scalings of the weight sequence S_R . Thus we can assume without loss of generality that $n_R \mathbb{E}[M_{R1}] = n_L \mathbb{E}[M_{L1}]$. This corresponds to the natural condition that the expected degree sum of the left and right side is equal.

A practical concern is how efficiently we can sample from this model, as naive sampling of the bipartite graph requires $n_L n_R$ coin flips. There are fast sampling heuristics for the bipartite graph, based on sampling each node in an edge individually for some pre-specified number of edges [3]. We develop a fast sampling algorithm in Section 4 that has some theoretical optimality guarantees for sequences S_L and S_R with certain properties.

2.2. Configuration models. Much of our motivation for random graph models is that they provide a baseline for what graph properties we might expect in network data just from a simple underlying random process (in our case, we are particularly interested in what graph properties we can expect from projection). In turn, this helps researchers determine which properties of the data are interesting or inherent to the system modeled by the graph.

While Chung-Lu models aim to preserve input degree sequences in expectation, *configuration models* preserve degrees exactly, sampling from the space of graphs with a specified degree sequence [25]. Configuration models for bipartite graphs have only been studied in earnest recently [17], where the goal is to sample bipartite graphs with a specified degree sequence for the left and right nodes. A bipartite configuration model inherits many benefits of a standard configuration model; for instance, the degree sequence is preserved exactly, creating an excellent null model for a given dataset.

At the same time, configuration models carry some restrictions. First, the random events on the existence of two edges are dependent (though weakly). To see this, in a stub-labeled bipartite graph, if we condition on an edge existing between $u \in L$ and $v \in R$, then there is one fewer stub for each node, making them less likely to connect to other nodes. This makes theoretical analysis difficult. Second, to generate a random graph, a configuration model needs a degree sequence that is realizable. While the Gale–Ryser theorem provides a simple way to check if a candidate bipartite degree sequence is realizable [48], configuration models typically analyze a given input graph rather than a class of input graphs with some property. Third, efficient uniform sampling algorithms rely on Markov Chain Monte Carlo, for which it is extremely difficult to obtain reasonable mixing time bounds.

The Chung-Lu approach (for either bipartite or unipartite graphs) sacrifices control over the exact degree sequence for easier theoretical analysis while maintaining the *expected* degree sequence. Unlike the configuration model, the existences of two distinct edges are independent

events, there is no need to specify a realizable degree sequence, and samples can be immediately generated. In unipartite graphs, this has led to remarkable results on random graphs with expected power-law degree sequences, such as small average node distance and diameter [18], the existence of a giant connected component [19], and spectral properties [20].

2.3. Related projection-based models. There are random graph models for bipartite graphs that are motivated by how the projection step can lose information about community structure in the data [30, 33]. While these identify possible issues with the projection, we are motivated by the fact that several datasets are constructed via projection, either implicitly or explicitly. There are also many models based on communities, where edge probabilities depend on community membership [2, 32, 50, 59]. These models can be interpreted as probabilistic projections of node-community bipartite graphs. Such models are typically fit from data to reveal cluster structure. Such analysis is not the focus of this paper.

There are a few random graph models where a random bipartite graph is deterministically projected [7, 17, 35, 58]. Some of these have specifically considered clustering, which is of primary interest for us. A recent example is the configuration model for hypergraphs [17], which can be interpreted as a bipartite random graph model: the nodes in the hypergraph are the left nodes in the bipartite graph, and the right nodes in the bipartite graph correspond to edges in the hypergraph. Chodrow [17] found that the clustering of projections of bipartite representations of several real-world hypergraph datasets was similar to or even less than the clustering of projections of samples from the configuration model. Similar empirical results have been found on related datasets, under a model that samples the degrees of the left nodes in the bipartite graph according to a distribution learned from the data and connects the edges to the right nodes uniformly at random [26]. Our theoretical analysis provides additional grounding for these empirical results, and our model provides a Chung-Lu-style alternative to the configuration model approach.

In terms of theoretical results, the models most related to ours are *random intersection graphs* [10, 27] and *random clique covers* [58]. In these models, a graph is constructed by sampling n sets from a universe of size m according to a distribution D . A node is associated to each of the n sets, and two vertices in the graph are adjacent if their subsets overlap. This is equivalent to representing the sets as an n -by- m bipartite graph and then projecting the graph onto the left nodes. Such models can also produce several key properties of projected graphs in practice, such as power-law degree distributions and negative correlation of clustering and projected degree. In contrast to these approaches, our model can specify degree distributions on both sides of the bipartite graph, as opposed to just one side. *Inhomogeneous random intersection graphs* also support arbitrary degree distribution on both sides [12, 13], and justify the negative correlation of local clustering and projected degree. In comparison, our analysis is conducted conditional on the degree sequence, which is potentially generated from a distribution with infinite moment, and thus requires a weaker and more realistic assumption on the degree distribution than results from Bloznelis and Petuchovas [11, 13]; however, their results work directly with projected degrees, which is advantageous.

3. Theoretical Properties of the Projection Model. In this section we provide results for graph statistics on the projected graph, such as the degree distribution, clustering coefficients, and closure coefficients. For intuition, one may think of the input weight distributions to our

model as the degree distribution of a class of input graphs. As we show in Section 5, these input weights often follow a power law distribution in real-world datasets. Due to the simplicity of our model, it is possible to derive analytical expressions when the input weight distribution follows a power law (Definition 1.4).

At a high-level, for a broad range of weight distributions (including power-law distributions), the projected graph has the following properties.

1. The projected graph is sparse (edge probabilities go to zero).
2. Expected local clustering at a node decays with the node's weight, and the node's weight is directly proportional to its degree in expectation.
3. Expected local closure at a node is the same for all nodes.
4. Global clustering and closure (transitivity) is a positive constant. In other words, clustering does not go to zero as the graph grows large.

Besides theoretical analysis, we also verify some key results with simulations, which relies on a fast sampling algorithm that we develop in section 4.

3.1. Assumptions on Weight Sequences. Our analysis is conditional on the general input weight sequence on both sides of the bipartite graph. We first assume that the normalized product of weights is at most one, making the edge existence probability (Equation (2.1)).

Assumption 1 (Well-defined probabilities). *The weight in the sequences S_L and S_R satisfy $\frac{w_u w_v}{n_R M_{R1}} \leq 1$ for any nodes $u \in L, v \in R$.*

Moreover, our analysis is asymptotic, meaning that the result holds with high accuracy on large networks, i.e., $n_L, n_R \rightarrow \infty$. For any two quantities f and g , we use the following big- O notations in the limit of $n_L, n_R \rightarrow \infty$: $f = o(g)$ if $f/g \rightarrow 0$; $f = O(g)$ if f/g is bounded; and $f = \Omega(g)$ if f/g is bounded away from 0. We make the following assumption on the range and moment of weight sequences.

Assumption 2 (Bounded weight sequences). *There exists a constant $\delta > 0$ such that*

- (bounded range) $\max[S_L, S_R] = O\left(n_R^{1/2-\delta}\right)$, $\min[S_L] = \Omega(1)$ and
- (bounded S_R moments) $M_{R2} = O(M_{R1}^2)$, $M_{R4} = O\left(n_R^{1-2\delta}\right)$,

as $n_L, n_R \rightarrow \infty$.

Assumption 2 actually specifies a family of assumptions parameterized by δ , with larger δ imposing stronger assumptions. Unless otherwise stated, we only require that $\delta > 0$. In the theoretical analysis of clustering coefficient, we sometimes require $\delta > 1/10$.

We do not assume the rate of which $n_L, n_R \rightarrow \infty$, or any direct relationships between n_L and n_R . This makes our assumptions weaker than a wide range of assumptions typical in the literature, such as having $n_L = \beta n_R^\sigma$ for certain $\beta, \sigma > 0$ [10, 13, 22, 58].

Before presenting the properties of bipartite or projected graph under these assumptions, we first show that these assumptions are naturally satisfied if the weight sequences are generated from the power-law distribution.

Proposition 3.1. *If the sequences S_L and S_R are independent generated from the power-law distribution with $w_{\max} = n_R^{1/2-\delta}$, and the right side distribution has decay exponent $\alpha_R > 3$, then Assumption 2 is satisfied.*

Proof. The bounded range requirement is automatically satisfied due to max capping, and we focus on the bounded moment requirement.

Let W be the random variable denoting a sample weight in S_R . Since $M_{R1} \geq 1$, due to the law of large numbers, it suffices to show that $\mathbb{E}[W^2] < \infty$ and $\mathbb{E}[W^4] = O(n_R^{1-2\delta})$ as $n_R \rightarrow \infty$. The first result can be easily verified, and when $\alpha_R \geq 5$, a straight-forward computation shows that $\mathbb{E}[W^4] = O(\log n_R)$. When $\alpha_R \in (3, 5)$, we have

$$\mathbb{E}[W^4] = \int_1^{n_R^{1/2-\delta}} C_{\alpha,\delta} \cdot w^{-\alpha+4} dw = \frac{C_{\alpha,\delta}}{(5-\alpha)} \left(n_R^{(5-\alpha)(\frac{1}{2}-\delta)} - 1 \right) = O\left(n_R^{1-2\delta}\right),$$

where $C_{\alpha,\delta} = (1 - n_R^{(1-\alpha)(1/2-\delta)})/(\alpha - 1) = O(1)$ is the normalizing constant. \blacksquare

Therefore, Assumption 2 is satisfied when the weight sequences are generated from power-law distributions with only a mild requirement on the decay exponent. In contrast, some results require constant weights on the right side [10, 22] or $\alpha_R > 5$ (for a finite fourth-order moment) [13].

When $M_{R1} \geq 1$, Assumption 1 is a direct consequence of Assumption 2 for large graphs since $\max[S_L, S_R] = o(\sqrt{n_R})$. Henceforth, for our theoretical analysis, we assume that both Assumption 1 and Assumption 2 are satisfied.

As a final note, a direct consequence of Assumption 2 is that $\mathbb{P}[(u, v) \in E_b \mid w_u, w_v] \rightarrow 0$ due to $w_u, w_v = o(n_R)$, meaning that the bipartite network is sparse.

3.2. Degree distribution in the bipartite graph. In this section, we study the degree distribution in the bipartite graph with respect to a given input weight distribution.

Theorem 3.2. *For any node $u \in L$, conditional on u 's weight w_u , the bipartite degree $d_b(u)$ of u converges in distribution to a Poisson random variable with mean w_u as $n_R \rightarrow \infty$. Analogously, for any $v \in R$, conditional on w_v , $d_b(v)$ converges in distribution to a Poisson random variable with mean w_v as $n_L \rightarrow \infty$.*

Proof. By symmetry, we just need to prove the result for a node $u \in L$. For any $v \in R$, the indicator function $\mathbb{1}_{[(u,v) \in E_b]}$ is a Bernoulli random variable with positive probability $\frac{w_u w_v}{n_R M_{R1}}$. By a Taylor expansion, its characteristic function can be written as

$$\phi_{uv}(t) = 1 + (e^{it} - 1) \frac{w_u w_v}{n_R M_{R1}} = e^{\frac{w_u w_v}{n_R M_{R1}} (e^{it} - 1) \cdot (1 + o(1))},$$

where the $o(1)$ term comes from the bounded range condition in Assumption 2. The bipartite degree of node u is the sum of the indicator functions of all nodes $v \in R$, which are independent random variables. Thus, its characteristic function of $d_b(u)$ can be written as

$$\phi_{d_b(u)}(t) = \prod_{v \in R} \phi_{uv}(t) = e^{w_u \frac{\sum_{v \in R} w_v}{n_R M_{R1}} (e^{it} - 1) \cdot (1 + o(1))} \rightarrow e^{w_u (e^{it} - 1)}.$$

The limiting characteristic function is the characteristic function of a Poisson random variable with mean w_u . Thus, $d_b(u)$ converges in distribution to a Poisson random variable with mean w_u by Lévy's continuity theorem. \blacksquare

One corollary of Theorem 3.2 is that, in the limit, the expected degree of any node u is its weight w_u , which provides an interpretation of the node weights. Next, we show that if the weights are independently generated from a power-law distribution, then the degrees in the bipartite graph are power-law distributed as well.

Theorem 3.3. *Suppose that the node weights on the left are independently sampled from a continuous power-law distribution with exponent α_L . Then, for any node $u \in L$, as $n_R \rightarrow \infty$, we have that $\mathbb{P}[d_b(u) = k] \propto k^{-\alpha_L}$ for large k .*

Similarly, suppose that the node weights on the right are independently sampled from a continuous power-law distribution with exponent α_R . Then, for any node $v \in R$, as $n_L \rightarrow \infty$, we have that $\mathbb{P}[d_b(v) = k] \propto k^{-\alpha_R}$ for large k .

Proof. Again, by symmetry, we only need to show the result for a node on the left. For any node $u \in L$, according to Theorem 3.2, its bipartite degree distribution converges to a Poisson distribution with mean w_u . For any integer $k > \alpha$,

$$\begin{aligned} \mathbb{P}[d_b(u) = k] &= \int_1^{w_{\max}} \mathbb{P}[d_b(u) = k \mid w_u = w] \cdot f_L(w) \, dw \\ &= C \int_1^{w_{\max}} e^{-w} \frac{w^k}{k!} \cdot w^{-\alpha_L} \, dw \\ &= \frac{C}{k!} \left(\int_0^\infty e^{-w} w^{k-\alpha_L} \, dw - \int_0^1 e^{-w} w^{k-\alpha_L} \, dw - \int_{w_{\max}}^\infty e^{-w} w^{k-\alpha_L} \, dw \right) \\ &= \frac{C}{\Gamma(k+1)} (\Gamma(k - \alpha_L + 1) - O(1)) \rightarrow Ck^{-\alpha_L} (1 + o(1)). \end{aligned}$$

Here, C is a normalizing constant. The second to last line is due to the fact that $w_{\max} = \Omega(1)$, and the last line follows because $\Gamma(k - \alpha_L + 1)/\Gamma(k + 1) \rightarrow k^{-\alpha_L}$ as $k \rightarrow \infty$. ■

3.3. Edge density and degree distribution in the projected graph. To study the edge density and degree distribution in the projected graph, we use the following quantity:

$$(3.1) \quad p_{u_1 u_2} := \frac{M_{R2}}{M_{R1}^2} \frac{w_{u_1} w_{u_2}}{n_R}.$$

The following theorem shows that $p_{u_1 u_2}$ is the asymptotic edge existence probability between the two nodes u_1 and u_2 in the *projected graph*. Note that under Assumption 2, we have $w_{u_1}, w_{u_2} = O(n_R^{1/2-\delta})$ and thus $p_{u_1 u_2} = O(n_R^{-2\delta}) = o(1)$, so the projected graph is sparse as the number of nodes goes to infinity.

Theorem 3.4. *For any $u_1, u_2 \in L$, as $n_R \rightarrow \infty$, we have*

$$\mathbb{P}[(u_1, u_2) \in E \mid S_L, S_R] = p_{u_1 u_2} - \frac{p_{u_1 u_2}^2}{2} + \left(\frac{p_{u_1 u_2}}{6} + \frac{M_{R4}}{2n_R M_{R2}^2} \right) p_{u_1 u_2}^2 \cdot (1 + O(n_R^{-2\delta})).$$

Proof. We consider the complementary case when u_1 and u_2 are not connected in the projected graph. This is the case when, for any nodes $v \in R$, it is connected to at most one

of u_1 and u_2 in the bipartite graph. For each single node $v \in R$, this case happens with probability $1 - \frac{w_{u_1} w_{u_2} w_v^2}{n_R^2 M_{R1}^2}$. Therefore,

$$\begin{aligned} \log(\mathbb{P}[(u_1, u_2) \notin E \mid S_L, S_R]) &= \sum_{v \in R} \log\left(1 - \frac{w_{u_1} w_{u_2} w_v^2}{n_R^2 M_{R1}^2}\right) \\ &= \sum_{v \in R} \left[-\frac{w_{u_1} w_{u_2} w_v^2}{n_R^2 M_{R1}^2} - \frac{w_{u_1}^2 w_{u_2}^2 w_v^4}{2n_R^4 M_{R1}^4} \cdot (1 + O(n_R^{-4\delta})) \right] = -p_{u_1 u_2} - \frac{M_{R4}}{2n_R M_{R2}^2} p_{u_1 u_2}^2 \cdot (1 + O(n_R^{-4\delta})). \end{aligned}$$

Consequently,

$$\mathbb{P}[(u_1, u_2) \in E \mid S_L, S_R] = p_{u_1 u_2} - \frac{p_{u_1 u_2}^2}{2} + \left(\frac{p_{u_1 u_2}}{6} + \frac{M_{R4}}{2n_R M_{R2}^2} \right) p_{u_1 u_2}^2 \cdot (1 + O(n_R^{-2\delta})). \quad \blacksquare$$

We now examine the expected degree distribution of the projected graph. One concern is the possibility of multi-edges in our definition of a projection, which occurs when two nodes $u_1, u_2 \in L$ have more than one common neighbor in the bipartite graph. The following lemma shows that the probability of having multi-edges conditional on edge existence is negligible, meaning that we can ignore the case of multi-edges with high probability.

Lemma 3.5. *Let $u_1, u_2 \in L$, and let $N_{u_1 u_2}$ be the number of common neighbors of u_1 and u_2 in the bipartite graph, then $\mathbb{P}[N_{u_1 u_2} \geq 2 \mid S_L, S_R, (u_1, u_2) \in E] = O(p_{u_1 u_2})$ as $n_R \rightarrow \infty$.*

Proof. Note that it suffices to show that $\mathbb{P}[N_{u_1 u_2} \geq 2 \mid S_L, S_R] = O(p_{u_1 u_2}^2)$. By the tail formula for expected values,

$$\begin{aligned} \mathbb{E}[N_{u_1 u_2} \mid S_L, S_R] &= \sum_{k=1}^{\infty} k \cdot \mathbb{P}[N_{u_1 u_2} = k \mid S_L, S_R] \\ &\geq 2 \cdot \mathbb{P}[N_{u_1 u_2} \geq 2 \mid S_L, S_R] + \mathbb{P}[N_{u_1 u_2} = 1 \mid S_L, S_R] \\ &= \mathbb{P}[N_{u_1 u_2} \geq 2 \mid S_L, S_R] + \mathbb{P}[N_{u_1 u_2} \geq 1 \mid S_L, S_R]. \end{aligned}$$

Note that we also have

$$\mathbb{E}[N_{u_1 u_2} \mid S_L, S_R] = \sum_{v \in R} \mathbb{P}[(u_1, v), (u_2, v) \in E_b \mid S_L, S_R] = p_{u_1 u_2},$$

and consequently

$$\mathbb{P}[N_{u_1 u_2} \geq 2 \mid S_L, S_R] \leq p_{u_1 u_2} - \mathbb{P}[N_{u_1 u_2} \geq 1 \mid S_L, S_R] \leq \frac{1}{2} p_{u_1 u_2}^2 + o(p_{u_1 u_2}^2).$$

The inequality uses the fact that the event $N_{u_1, u_2} \geq 1$ is equivalent to the existence of edge (u_1, u_2) in the projected graph, which happens with probability $p_{u_1 u_2} - \frac{1}{2} \cdot p_{u_1 u_2}^2 + o(p_{u_1 u_2}^2)$ by Theorem 3.4. \blacksquare

Now we are ready to analyze the degree of a node in the projected graph. The following theorem says that degree of a node in the projected is directly proportional the weight of the node. Thus, at least in expectation, we can think of the weight as a proxy for degree.

Theorem 3.6. *For any $u \in L$, as $n_L, n_R \rightarrow \infty$, we have*

$$\mathbb{E}[d(u) \mid S_L, S_R] = \frac{M_{R2} M_{L1}}{M_{R1}^2} \cdot \frac{n_L}{n_R} \cdot w_u \cdot (1 + o(1)),$$

Proof. By Theorem 3.4,

$$\begin{aligned} \mathbb{E}[d(u) \mid S_L, S_R] &= \sum_{u_1 \in L, u_1 \neq u} \mathbb{P}[(u, u_1) \in E \mid S_L, S_R] = \sum_{u_1 \in L, u_1 \neq u} \frac{w_u w_{u_1}}{n_R} \cdot \frac{M_{R2}}{M_{R1}^2} \cdot (1 + o(1)) \\ &= \frac{M_{R2} M_{L1}}{M_{R1}^2} \cdot \frac{n_L}{n_R} \cdot w_u \cdot (1 + o(1)). \quad \blacksquare \end{aligned}$$

By Theorem 3.3, the bipartite degree distributions of the left and right nodes are power-law distributions with exponents α_L and α_R . For such bipartite graphs, Nacher and Aktsu [38] showed that the degree sequence of the projected graph follows a power law distribution.

Corollary 3.7 (Section 2, [38]). *Suppose the node weights on the left and right follow power-law distributions with exponents α_L and α_R . Then the degree distribution of the projected graph is a power-law distribution with decay exponent $\min(\alpha_L, \alpha_R - 1)$.*

When $\alpha_R \in (3, 4)$, Assumption 2 is satisfied by Proposition 3.1, and the projected graph would have power-law degree distribution with decay exponent within $(2, 3)$, which is a standard range for classical theoretical models [23] and is also observed in real-world data [15]. We estimate $\alpha_R \in (3, 4)$ for several real-world bipartite networks that we analyze (Appendix B).

3.4. Clustering in the projected graph. In this section we compute the expected value of the clustering and closure coefficients. Theorem 3.8 rigorously analyzes the expected value of local clustering coefficients on networks generated from projections of general bipartite random graphs. Our results show how (for a broad class of random graphs) the expected local clustering coefficient varies with the node weight: it decays at a slower rate for small weight and then decays as the inverse of the weight for large weights. Combined with the result that the expected projected degree is proportional to the node weight (Theorem 3.6), this says that there is an inverse correlation of node degree with the local clustering coefficient, which we also verify with simulation. This has long been a noted empirical property of complex networks [41], and our analysis provides theoretical grounding, along with other recent results [11, 13].

Theorem 3.8. *If Assumption 2 is satisfied with $\delta > \frac{1}{10}$, then conditioned on S_L and S_R for any node $u \in L$, we have in the projected graph that*

$$C(u) = \frac{1}{1 + \frac{M_{R2}^2}{M_{R3}M_{R1}} w_u} + o(1).$$

Besides the trend of how local clustering coefficient decays with node weight, we highlight how the sequence moment of S_R influences the clustering coefficient. If the distribution of S_R has a heavier tail, then $\frac{M_{R2}^2}{M_{R3}M_{R1}}$ is small (via Cauchy-Schwartz), and one would expect higher local clustering compared to cases where S_R is light-tailed [13] or uniform [10, 22]. We also observe this higher level of clustering in simulations (Figure 5.1).

We break the proof of Theorem 3.8 into several lemmas. From this point on, we assume $\delta > 1/10$. We first present the following results on the limiting probability of wedge and triangle existence, with proofs given in Appendix C.

Lemma 3.9. *As $n_R \rightarrow \infty$, for any node triple (u_1, u, u_2) , the probability that they form a wedge centered at u is*

$$\mathbb{P}[(u, u_1), (u, u_2) \in E \mid S_L, S_R] = \left(1 + \frac{M_{R1}M_{R3}}{M_{R2}^2} \cdot \frac{1}{w_u}\right) p_{uu_1}p_{uu_2} \cdot (1 + o(1)).$$

Lemma 3.10. *In the limit of $n_R \rightarrow \infty$, the probability of a node triple (u_1, u, u_2) forms a triangle is*

$$\mathbb{P}[(u, u_1), (u, u_2), (u_1, u_2) \in E \mid S_L, S_R] = p_{uu_1}p_{uu_2} \cdot \frac{M_{R1}M_{R3}}{M_{R2}^2} \cdot \frac{1}{w_u} \cdot (1 + o(1)) + o(p_{uu_1}p_{uu_2}).$$

Now we have the following key result on the conditional probability triadic closure.

Lemma 3.11. *In the limit of $n_L, n_R \rightarrow \infty$, if a node triple (u_1, u, u_2) forms an wedge, then the probability of this wedge being closed is*

$$\mathbb{P}[(u_1, u_2) \in E \mid S_L, S_R, (u, u_1), (u, u_2) \in E] = \frac{1}{1 + \frac{M_{R2}^2}{M_{R3}M_{R1}}w_u} + o(1).$$

Proof. By combining the result of Lemmas 3.9 and 3.10, we have

$$\begin{aligned} \mathbb{P}[(u_1, u_2) \in E \mid S_L, S_R, (u, u_1), (u, u_2) \in E] &= \frac{\mathbb{P}[(u, u_1), (u, u_2), (u_1, u_2) \in E \mid S_L, S_R]}{\mathbb{P}[(u, u_1), (u, u_2) \in E \mid S_L, S_R]} \\ &= \frac{p_{uu_1}p_{uu_2} \frac{M_{R1}M_{R3}}{M_{R2}^2} \cdot \frac{1}{w_u} \cdot (1+o(1)) + o(p_{uu_1}p_{uu_2})}{\left(\frac{M_{R1}M_{R3}}{M_{R2}^2} \cdot \frac{1}{w_u} + 1\right) p_{uu_1}p_{uu_2} \cdot (1+o(1))} = \frac{1+o(1)}{1 + \frac{M_{R2}^2}{M_{R3}M_{R1}}w_u} + o(1). \quad \blacksquare \end{aligned}$$

Finally, we are ready to prove our main result.

Proof of Theorem 3.8. According to Equation (1.2), the local clustering coefficient is the conditional probability that a randomly chosen wedge centered at node u forms a triangle. Lemma 3.11 shows that this probability is asymptotically the same regardless of the weights on the wedge endpoints u_1, u_2 . Therefore conditioned on S_L and S_R , we have

$$C(u) = \mathbb{P}[(u_1, u_2) \in E \mid S_L, S_R, (u, u_1), (u, u_2) \in E] = \frac{1}{1 + \frac{M_{R2}^2}{M_{R3}M_{R1}}w_u} + o(1). \quad \blacksquare$$

Figure 3.1 shows the mean conditional local clustering coefficient of a projected graph as a function of node weights w_u for networks where $n_L = n_R = 10,000,000$ and weights drawn from discrete power-law distributions with different decay parameters. We cap the maximum value of the weights at $n_L^{0.3}$, which corresponds to $\delta = 0.2$ in Assumption 2. The empirical clustering is close to the expected value from Theorem 3.8.

We can also analyze the global clustering coefficient (also called the *transitivity*) of the projected graph. The following theorem says that the global clustering tends to a constant bounded away from 0.

Theorem 3.12. *If Assumption 2 is satisfied with $\delta > \frac{1}{10}$, then conditioned on S_L and S_R , we have in the projected graph that*

$$C_G = \frac{1}{1 + \frac{M_{R2}^2}{M_{R3}M_{R1}} \cdot \frac{M_{L2}}{M_{L1}}} + o(1).$$

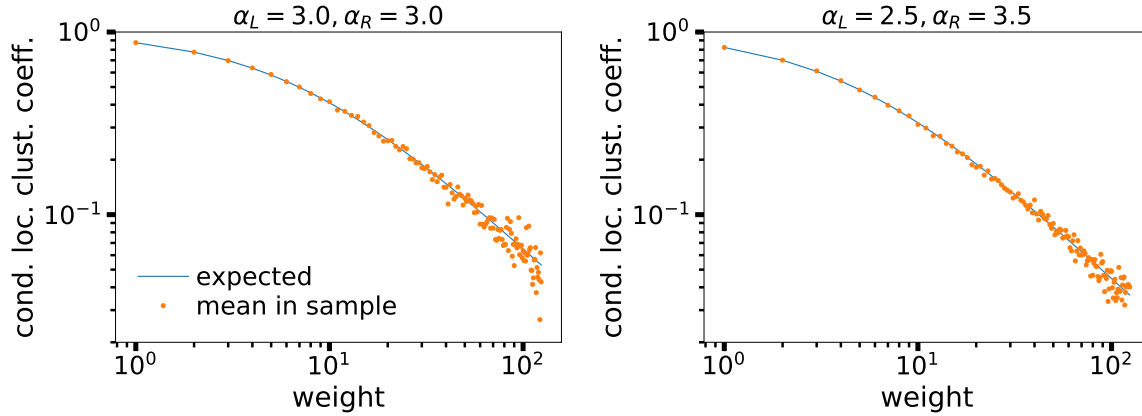


Figure 3.1: Conditional local clustering coefficient distribution on simulated graphs as a function of node weight w_u , where left and right node weights are sampled from a discrete power law distribution with decay rates α_L and α_R . The dots are the mean conditional local clustering coefficients for all nodes with that weight, and the curve is the prediction from Theorem 3.8.

Proof. Let \mathcal{W} be the set of wedges in G and \mathcal{T} be the set of triangles. We first show that the global clustering coefficient is always well-defined, i.e. $\mathbb{P}[|\mathcal{W}| \geq 1] \geq 1 - \exp(-O(n_R))$. We show that with high probability, some node on the right partition has degree at least 3. This implies that a triangle exists in the graph and therefore a wedge exists. For any given node v on the right, its expected degree is w_v by Theorem 3.2 and the degrees follow a Poisson distribution. By standard concentration bounds [16], $\mathbb{P}[d_b(u) \leq 2] \leq \exp(-w_v/4)$ for w_v larger than 2 (in particular, this probability is less than $1/3$ when $w_v > 7$). Thus, given the mild assumption that the weights have finite support for weights larger than 7, the probability that there exists at least 1 triangle is $1 - (\frac{1}{3})^{O(n_R)}$.

Next, we note that the probabilities computed in Lemma 3.11 remain unchanged when conditioned on the fact that at least one wedge exists. Let E be the event that some wedge (u, u_0, u_1) closes into a triangle (with u as the centre of the wedge).

$$\mathbb{P}[E \cap |\mathcal{W}| \geq 1] \geq \mathbb{P}[E] - (1 - \mathbb{P}[|\mathcal{W}| \geq 1]) = \mathbb{P}[E] - \left(\frac{1}{3}\right)^{O(n_R)},$$

Consequently,

$$\mathbb{P}[E] - \left(\frac{1}{3}\right)^{O(n_R)} \leq \mathbb{P}[E \mid |\mathcal{W}| \geq 1] \leq \mathbb{P}[E] + \left(\frac{1}{3}\right)^{O(n_R)}.$$

Finally, $\mathbb{P}[E] = \Omega(n_R^{O(1)})$ for any of the events we previously considered, so the exponentially small deviation does not produce any additional error in our results.

For any node u , the probability that a random wedge has center u is proportional to the number of wedges centred at u . By our reasoning above, we can assume at least 1 wedge

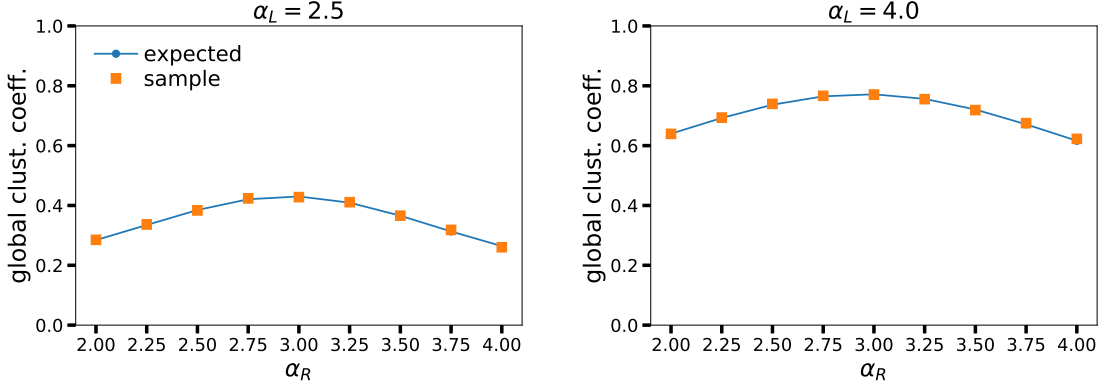


Figure 3.2: Expected (via Theorem 3.12) and sampled global clustering coefficients on simulated graphs with discrete power law weight distributions on the left and right nodes with decay rights α_L and α_R . The samples are close to the expected value.

exists, so these probabilities sum to 1. By Lemma 3.11, we have:

$$\mathbb{P}[u \text{ is the center node}] = \frac{\sum_{b,c \in L} \left(1 + \frac{M_{R1}M_{R3}}{M_{R2}^2} \cdot \frac{1}{w_u}\right) \cdot p_{ub}p_{uc}}{\sum_{a,b,c \in L} \left(1 + \frac{M_{R1}M_{R3}}{M_{R2}^2} \cdot \frac{1}{w_a}\right) p_{ab}p_{ac}} + o(1).$$

Putting everything together,

$$C_G = \sum_{u \in L} \mathbb{P}[(u, u_1, u_2) \in \mathcal{T} \mid (u, u_1, u_2) \in \mathcal{W}] \cdot \mathbb{P}[u \text{ is the center}] = \frac{1}{1 + \frac{M_{R2}^2}{M_{R3}M_{R1}} \cdot \frac{M_{L2}}{M_{L1}}} + o(1),$$

where the probability is taken over all $u_1, u_2 \in L$ and the second equality uses Lemma 3.11 for the probability that $(u, u_1, u_2) \in \mathcal{T}$. \blacksquare

Figure 3.2 shows the expected (computed from Theorem 3.12) and actual global clustering coefficient of the projected graph with $n_L = n_R = 1,000,000$. The weights are drawn from a discrete power law distribution with fixed decay rate $\alpha_L = 2.5$ or 4.0 on the left nodes, varying decay rate α_R on the right nodes, and $w_{\max} = n_L^{0.5}$. The sampled global clustering coefficients are close to the expectation at all parameter values.

Finally, we investigate the local closure coefficient $H(u)$. Analysis under the configuration model predicts that $H(u)$ should be proportional to the node degree, while empirical analysis demonstrates a much slower increasing trend versus degree, or even a constant relationship in a coauthorship network that is directly generated from the bipartite graph projection [60]. The following result theoretically justify this phenomenon, showing the the expected value of local closure coefficient is independent from node weight

Theorem 3.13. *If Assumption 2 is satisfied with $\delta > \frac{1}{10}$, then conditioned on S_L and S_R we have, in the projected graph,*

$$H(u) = \frac{1}{1 + \frac{M_{R2}^2}{M_{R3}M_{R1}} \cdot \frac{M_{L2}}{M_{L1}}} + o(1)$$

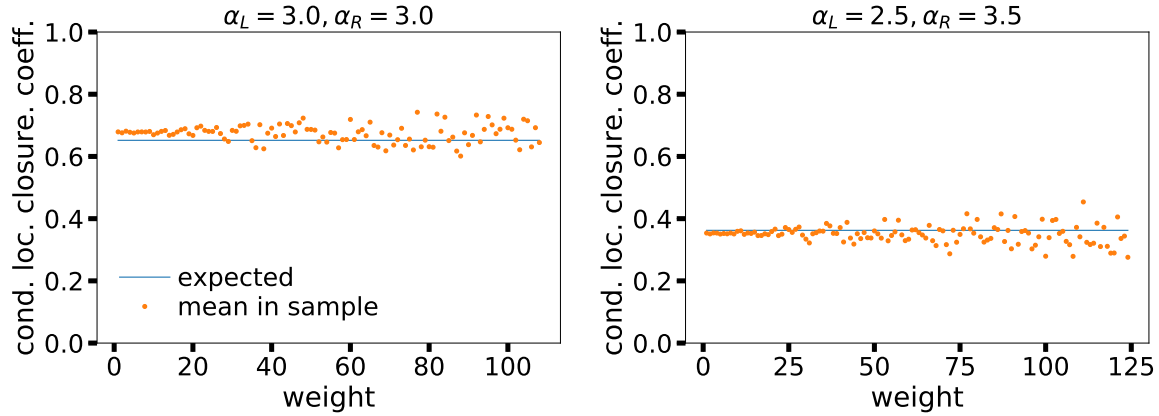


Figure 3.3: Conditional local closure coefficient distribution on simulated graphs as a function of node weight w_u , where left and right node weights are sampled from a discrete power law distribution with decay rates α_L and α_R . The dots are the mean conditional local closure coefficients for all nodes with that weight, and the flat curve is the prediction from Theorem 3.13. Weights with fewer than 5 nodes were omitted.

as $n_R \rightarrow \infty$, i.e., the expected closure coefficient is asymptotically independent of node weight.

Proof. By Theorem 3.8, the probability that a length-2 path (u, v, w) closes into a triangle only depends on its center node v . Since the closure coefficient is measured from the head node u , the probability that any wedge is closed is independent of u and thus the same across every node in the graph. This implies that the local closure coefficient is equal to the global closure coefficient, which in turn is equal to the global clustering coefficient. ■

Figure 3.3 shows the local closure coefficient of the projected graph as a function of node weights w_u , using the same random graphs as for the clustering coefficient in Figure 3.1. We observe that the mean local conditional closure coefficient is independent of the node weight in the samples, which verifies Theorem 3.13.

Remark 3.14. One can strengthen the error bounds in Theorems 3.8, 3.12, and 3.13 by assuming $\delta > 1/6$. In particular, instead of an additive $o(1)$ error term, the error terms are a multiplicative $1 + o(1)$ factor. For example, the global clustering coefficient in Theorem 3.12 would be

$$C_G = \frac{1}{1 + \frac{M_{R2}^2}{M_{R3}M_{R1}} \cdot \frac{M_{L2}}{M_{L1}}}(1 + o(1)).$$

4. Fast sampling and counting. We develop a fast sampling algorithm for graphs with degrees following discrete power law (Zipfian) distributions, which we use in all of our experiments. One naive way to implement our model is to simply iterate over all $O(n_L n_R)$ potential edges, and generate a random sample for each edge. For large graphs however, this quadratic scaling is too costly. In contrast, our algorithm has running time linear in the number of sampled edges rather than the product of the left and right partition sizes. This speedup is enabled by the discrete power law distributions, which allows us to group nodes with the same weight. The overall procedure is in Algorithm 4.1.

Algorithm 4.1 Fast sampling of a Chung-Lu bipartite graph with discrete power-law weights.

Input: positive integers n_L, n_R , and degree distributions D_L and D_R
Output: a bipartite graph G following degree distributions D_L and D_R
 $L \leftarrow \{1, 2, \dots, n\}, R \leftarrow \{n+1, n+2, \dots, n+n_R\}$
 $W_L \leftarrow \{w_u \mid w_u \sim D_L\}, W_R \leftarrow \{w_u \mid w_u \sim D_R\}$
 $G \leftarrow$ an empty graph with node set $L \sqcup R$
for each unique value $(w_l, w_r) \in W_L \times W_R$ **do**
 $V_L \leftarrow \{u \in L \mid w_u = w_l\}, V_R \leftarrow \{u \in R \mid w_u = w_r\}$
 $m \leftarrow |V_L||V_R|, p = \frac{w_l w_r}{n_R \mu_R}$
 $e_g \sim \text{Binomial}(m, p)$
 draw e_g uniformly from $V_L \times V_R$ without replacement and add them to G
end for
return G

Suppose that we have two discrete power law distributions D_L and D_R , with $n_L \mathbb{E}[D_L] = n_R \mathbb{E}[D_R]$ and decay parameters α_L and α_R . We begin by first sampling the node weights $w_u \in \mathbb{N}$ according to the specified distributions. We then group together nodes on each side of the bipartite graph by their weight. With high probability, the number of groups will be small (Lemma 1.5). Thus, instead of iterating over all $O(n_L n_R)$ pairs of potential edges, we can iterate over all pairs of groups between the left and right partition. Within each group, edges between nodes of the group occur with a fixed probability. Hence, the number of edges within the group follows a binomial distribution. The final step simply generates the number of edges e_g we need from each group, and then draws that many edges from the node pairs within that group, which can be done in linear time.

Theorem 4.1. *Let $\mu_L = \mathbb{E}[D_L]$ and $\mu_R = \mathbb{E}[D_R]$. The expected running time of Algorithm 4.1 is $O\left(n_L^{1/(\alpha_L-1)} n_R^{1/(\alpha_R-1)} + \mu_L n_L\right)$. For $\alpha_L, \alpha_R > 3$, the latter term dominates and the algorithm is asymptotically optimal since the second term is the expected number of edges.*

Proof. By Lemma 1.5, the $\mathbb{E}[|W_L|]$ and $\mathbb{E}[|W_R|]$ are $O\left(n_L^{1/(\alpha_L-1)}\right)$ and $O\left(n_R^{1/(\alpha_R-1)}\right)$. Thus, the number of unique pairs (w_u, w_v) iterated over in the for loop of Algorithm 4.1 is $O\left(n_L^{1/(\alpha_L-1)} n_R^{1/(\alpha_R-1)}\right)$ in expectation. Aside from the time taken to draw e_g edges, each group takes constant time to process. The expected number of edges added over all the groups is $\sum_{u \in L, v \in R} \frac{w_u w_v}{n_R \mu_R} = n_L M_{1L}$. This tends to $O(n_L \mu_L)$ in expectation. Hence the total running time is upper bounded by $O\left(n_L^{1/(\alpha_L-1)} n_R^{1/(\alpha_R-1)} + \mu_L n_L\right)$.

Following Remark 2.1, we may assume without loss of generality that $\mu_L n_L = \mu_R n_R$. By the AM-GM inequality, $\frac{\mu_L n_L + \mu_R n_R}{2} \geq \sqrt{n_L n_R \mu_L \mu_R}$. For $\alpha_L, \alpha_R \geq 3$, the latter term dominates and the runtime is bounded by the expected number of generated edges. Since the output size is at least $O(\mu_L n_L)$, Algorithm 4.1 is asymptotically optimal when $\alpha_L, \alpha_R \geq 3$. ■

Next, we analyze the complexity of computing the graph projection along with several of the network statistics we have considered.

Lemma 4.2. *Let D_L and D_R with decay parameters α_L and α_R be the weight distributions. In expectation, the running time for computing all local clustering and closure coefficients and*

the global clustering coefficient is $O\left(n_L^{1/\min(\alpha_L, \alpha_R - 1)} \frac{n_L^2 M_{1L}^2 M_{R2}}{n_R M_{1R}^2}\right)$. Under the normalization in Remark 2.1, this is equal to $O\left(n_L^{1/(\alpha_L - 1)} n_R^{1/(\alpha_R - 1)} + \mu_L n_L + \mu_R n_R\right)$. For $\alpha_L, \alpha_R > 3$, the algorithm is asymptotically optimal, since the second term is the expected number of edges.

Proof. To compute the projected graph, we can simply iterate over all nodes u in the right partition. For each pair of nodes in $N(u)$, we connect the nodes with an edge in the projected graph. Summed over all nodes in the right partition, we add $\sum_{v \in R} \left(\frac{n_L M_{1L}}{n_R M_{1R}} w_v\right)^2$ edges in the projected graph on expectation. Hence both the expected time to compute the projection and the expected number of edges in the projection is upper bounded by $O\left(\frac{n_L^2 M_{1L}^2 M_{R2}}{n_R M_{1R}^2}\right)$.

To compute the local clustering and closure coefficients, as well as the global clustering coefficient, it is sufficient to have the degree and triangle participation counts of each node. The degrees are immediately available from the projected graph, and we can list all triangles in $O(mn^{1/\alpha})$ time, where m is the number of edges in the projection, and α is the power law parameter of the projection [34]. By Corollary 3.7 and our reasoning above, $m = O\left(\frac{n_L^2 M_{1L}^2 M_{R2}}{n_R M_{1R}^2}\right)$ and $\alpha = \min(\alpha_L, \alpha_R - 1)$.

By Remark 2.1, it's convenient to interpret D_L and D_R as the degree distributions of the left and right partitions respectively. In these cases, we have the equality $n_L \mathbb{E}[D_L] = n_R \mathbb{E}[D_R]$. With this equality, our results above simplify. The running time of Algorithm 4.1 can be restated as $O\left(n_L^{1/(\alpha_L - 1)} n_R^{1/(\alpha_R - 1)} + \mu_L n_L + \mu_R n_R\right)$. Thus for $\alpha_L, \alpha_R > 3$, the latter terms dominate (by the AM-GM inequality) and the running time is asymptotically optimal, since it is bounded by the expected number of generated edges. ■

5. Numerical experiments. In this section, we use our model in conjunction with several datasets. We find that much of the empirical clustering behavior in real-world projections can be accounted for by our bipartite project model. All algorithms and simulations were implemented in C++, and all experiments were executed on a dual-core Intel i7-7500U 2.7 GHz CPU with 16 GB of RAM. Code and data are available at <https://gitlab.com/paul.liu.ubc/bipartite-generation-model>.

We analyze 11 bipartite network datasets (Table 5.1). For the weight sequences S_L and S_R , we use the degrees from the data. We also compare with a version of the random intersection model [10, 27], where the weight sequence of the left nodes comes from the data. For each dataset, we estimated power-law decay parameters for the degree distribution of the left and right partition (Appendix B).

Table 5.2 shows clustering and closure coefficients — mean local clustering (i.e., average clustering coefficient), global clustering (equal to global closure), and mean local closure (i.e., average closure coefficient) — from (1) the data, (2) the projected graph produced by our model, and (3) the graph produced by the random intersection model. When computing the coefficients, we ignore any node that has an undefined coefficient, and we report the empirical (i.e., non-conditional) variants defined in Subsection 1.1.

In all but one dataset, our model has mean local clustering that is closer to the data than the random intersection model. This remains true regardless of whether our model has more clustering (e.g., *mathsx-tags-questions*) or less clustering (e.g., *actors-movies*) compared to

Table 5.1: Description and summary statistics of real world datasets.

dataset	$ L $	$ R $	$ E_b $	projection description
actors-movies [6]	384K	128K	1.47M	actors in the same movie
amazon-products-pages [36]	721K	549K	2.34M	products displayed on the same page on <code>amazon.com</code>
classes-drugs [8]	1.16K	49.7K	156K	FDA NDC classification codes describing the same drug
condmat-authors-papers [40]	16.7K	22.0K	58.6K	academics co-authoring a paper on the Condensed Matter arXiv
directors-boards [49]	204	1.01K	1.13K	directors on the boards of the same Norwegian company
diseases-genes [28]	516	1.42K	3.93K	diseases associated with the same gene
genes-diseases [28]	1.42K	516	3.93K	genes associated with the same disease
mathsx-tags-questions [8]	1.63K	822K	1.80M	tags applied to the same question on <code>math.stackexchange.com</code>
mo-questions-users [55]	73.9K	5.45K	132K	questions answered by the same user
so-users-threads [8]	2.68M	11.3M	25.6M	users posting on the same question thread on <code>stackoverflow.com</code>
walmart-items-trips [5]	88.9K	69.9K	460K	items co-purchased in a shopping trip

Table 5.2: Clustering and closure coefficients in real-world data and in random projections following our model and the random intersection (RI) model. Variances are on the order of 0.001. A large amount clustering is simply explained by the degree distribution and projection.

dataset	mean clust. coeff.			global clust. coeff.			mean closure coeff.		
	data	ours	RI	data	ours	RI	data	ours	RI
actors-movies	0.78	0.63	0.58	0.17	0.07	0.04	0.20	0.04	0.03
amazon-products-pages	0.74	0.52	0.53	0.20	0.08	0.08	0.29	0.09	0.09
classes-drugs	0.83	0.79	0.78	0.50	0.50	0.49	0.40	0.24	0.23
condmat-authors-papers	0.74	0.50	0.50	0.36	0.12	0.11	0.35	0.10	0.10
directors-boards	0.45	0.28	0.34	0.39	0.21	0.23	0.27	0.17	0.19
diseases-genes	0.82	0.46	0.36	0.63	0.31	0.19	0.52	0.21	0.14
genes-diseases	0.86	0.65	0.57	0.66	0.37	0.23	0.54	0.24	0.19
mathsx-tags-questions	0.63	0.79	0.80	0.33	0.46	0.47	0.17	0.25	0.27
mo-questions-users	0.86	0.78	0.64	0.63	0.45	0.19	0.37	0.24	0.19
so-users-threads	0.40	0.45	0.46	0.02	0.01	0.01	0.00	0.01	0.01
walmart-items-trips	0.63	0.55	0.52	0.05	0.04	0.04	0.07	0.02	0.02

the data. The one exception is the *directors-boards* dataset, where the random intersection model accounts for more clustering than our model. In an absolute sense, a large amount of the mean clustering is created by the projection.

To further highlight how much is explained by our model, Figure 5.1 shows the local clustering coefficient as a function of degree in the data and in a sample from the models.

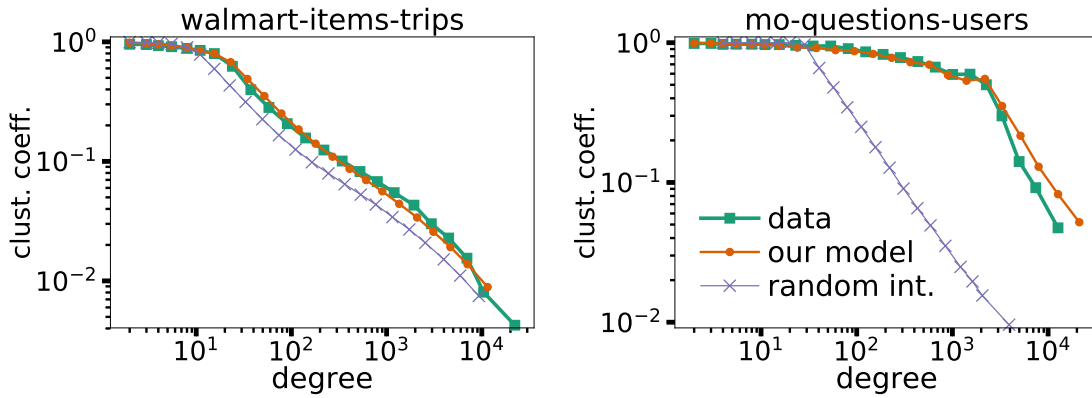


Figure 5.1: Local clustering coefficient as a function of degree on the *walmart-items-trips* (left) and *mo-questions-users* (right) datasets. The green, orange, and blue lines represent the clustering coefficients from the real projected graph, the projected graph produced by our model, and the projected graph produced by the random intersection model respectively. Much of the empirical local clustering behavior can be explained by the projection.

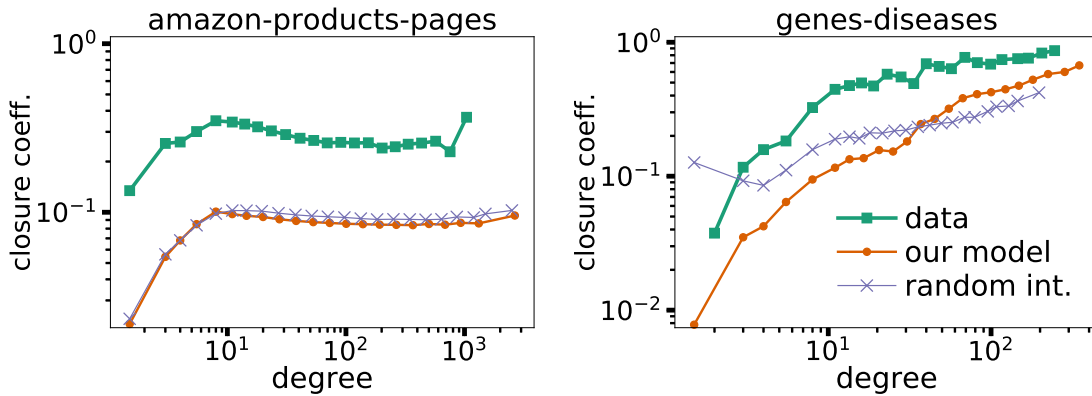


Figure 5.2: Local closure coefficient as a function of degree on the *walmart-items-trips* (left) and *genes-diseases* (right) datasets. The green, orange, and blue lines represent the clustering coefficients from the real projected graph, the projected graph produced by our model, and the projected graph produced by the random intersection model respectively.

We find that the empirical characteristics of the clustering coefficient as a function of degree are largely explained by the projection, suggesting that there is little innate local clustering behavior beyond what the projection from the degree distribution already provides.

In some datasets, the global clustering coefficient is essentially the same as in our model (*classes-drugs*, *walmart-items-trips*). However, there are several cases where our model and the random intersection model have a factor of two less global clustering (*actors-movies*, *amazon-products-pages*, *diseases-genes*). This suggests that there is global transitivity in these networks that goes beyond what we would expect from a random projection. Overall, the relative difference between the data and the model is larger for the global clustering coefficient

than for the local clustering coefficient. We emphasize that our model is not designed to match these empirical properties. Instead, we are interested in how much clustering one can expect from a model that only accounts for the bipartite degree distributions and the projection step.

Finally, the random graphs have non-trivial mean closure coefficients, but they tend to be smaller compared to the data, with the exception of *mathsx-tags-questions*. Similar to the local clustering coefficient, we plot the local closure coefficient as a function of degree for two datasets (*amazon-products-pages* and *genes-diseases*; Figure 5.2). For *amazon-products-pages*, we see the flat closure coefficient as one might expect from Theorem 3.13, although the data has more closure at baseline. This is likely explained by the fact that two products tend to appear on the same pages, reducing the number of length-2 paths in the data, whereas bipartite connections are made at random in the model. With the *genes-diseases* dataset, the random models capture an increase in closure as a function of degree that is also seen in the data. In this case, the model parameters do not satisfy the assumptions of Theorem 3.13, but the general empirical behavior is still seen in our random projection model.

6. Conclusion. We have analyzed a simple bipartite “Chung-Lu style” model that captures some common properties of real-world networks. The simplicity of our model enables theoretical analysis of properties of the projected graph, giving analytical formulae for graph statistics such as clustering coefficients, closure coefficients, and the expected degree distribution. We also pair our model with a fast optimal graph generation algorithm, which is provably optimal for certain input distributions. Empirically, we find that a substantial amount of clustering and closure behavior in real-world networks is explained by sampling from our model with the same bipartite degree distribution. However, global clustering is often larger than predicted by the projection model.

Acknowledgments. This research was supported by NSF Award DMS-1830274, ARO Award W911NF19-1-0057, ARO MURI, and JPMorgan Chase & Co. We thank Johan Ugander for pointing us to the literature on random intersection graphs.

REFERENCES

- [1] Y.-Y. AHN, S. E. AHNERT, J. P. BAGROW, AND A.-L. BARABÁSI, *Flavor network and the principles of food pairing*, Scientific Reports, 1 (2011).
- [2] E. M. AIROLDI, D. M. BLEI, S. E. FIENBERG, AND E. P. XING, *Mixed membership stochastic blockmodels*, Journal of machine learning research, 9 (2008), pp. 1981–2014.
- [3] S. G. AKSOY, T. G. KOLDA, AND A. PINAR, *Measuring and modeling bipartite graphs with community structure*, Journal of Complex Networks, 5 (2017), pp. 581–603.
- [4] J. ALSTOTT, E. BULLMORE, AND D. PLENZ, *powerlaw: a python package for analysis of heavy-tailed distributions*, PLoS one, 9 (2014), p. e85777.
- [5] I. AMBURG, N. VELDT, AND A. R. BENSON, *Clustering in graphs and hypergraphs with categorical edge labels*, in Proceedings of the Web Conference, 2020.
- [6] A.-L. BARABÁSI AND R. ALBERT, *Emergence of scaling in random networks*, Science, 286 (1999), pp. 509–512.
- [7] D. BARBER, *Clique matrices for statistical graph decomposition and parameterising restricted positive definite matrices*, in Proceedings of the Twenty-Fourth Conference on Uncertainty in Artificial Intelligence, AUAI Press, 2008, pp. 26–33.
- [8] A. R. BENSON, R. ABEBE, M. T. SCHAUB, A. JADBABAIE, AND J. KLEINBERG, *Simplicial closure and higher-order link prediction*, Proceedings of the National Academy of Sciences, 115 (2018),

- pp. E11221–E11230.
- [9] A. R. BENSON, D. F. GLEICH, AND J. LESKOVEC, *Higher-order organization of complex networks*, Science, 353 (2016), pp. 163–166.
 - [10] M. BLOZNELIS, *Degree and clustering coefficient in sparse random intersection graphs*, The Annals of Applied Probability, 23 (2013), pp. 1254–1289.
 - [11] M. BLOZNELIS, *Local probabilities of randomly stopped sums of power-law lattice random variables*, Lithuanian Mathematical Journal, 59 (2019), pp. 437–468.
 - [12] M. BLOZNELIS AND V. KURASUKAS, *Clustering coefficient of random intersection graphs with infinite degree variance*, Internet Mathematics, (2016), p. 1215.
 - [13] M. BLOZNELIS AND J. PETUCHOVAS, *Correlation between clustering and degree in affiliation networks*, in International Workshop on Algorithms and Models for the Web-Graph, Springer, 2017, pp. 90–104.
 - [14] R. L. BREIGER, *The duality of persons and groups*, Social forces, 53 (1974), pp. 181–190.
 - [15] A. D. BROIDO AND A. CLAUSET, *Scale-free networks are rare*, Nature communications, 10 (2019), pp. 1–10.
 - [16] C. CANNONE, *A short note on poisson tail bounds*. <http://www.cs.columbia.edu/~ccannonne/files/misc/2017-poissonconcentration.pdf>.
 - [17] P. S. CHODROW, *Configuration models of random hypergraphs*, arXiv:1902.09302, (2019).
 - [18] F. CHUNG AND L. LU, *The average distances in random graphs with given expected degrees*, Proceedings of the National Academy of Sciences, 99 (2002), pp. 15879–15882.
 - [19] F. CHUNG AND L. LU, *Connected components in random graphs with given expected degree sequences*, Annals of combinatorics, 6 (2002), pp. 125–145.
 - [20] F. CHUNG, L. LU, AND V. VU, *The spectra of random graphs with given expected degrees*, Internet Mathematics, 1 (2004), pp. 257–275.
 - [21] A. CLAUSET, C. R. SHALIZI, AND M. E. NEWMAN, *Power-law distributions in empirical data*, SIAM Review, 51 (2009), pp. 661–703.
 - [22] M. DEIJFEN AND W. KETS, *Random intersection graphs with tunable degree distribution and clustering*, Probability in the Engineering and Informational Sciences, 23 (2009), pp. 661–674.
 - [23] S. N. DOROGOVITSEV AND J. F. MENDES, *Evolution of networks*, Advances in physics, 51 (2002), pp. 1079–1187.
 - [24] D. EASLEY AND J. KLEINBERG, *Networks, crowds, and markets*, vol. 8, Cambridge university press Cambridge, 2010.
 - [25] B. K. FOSDICK, D. B. LARREMORE, J. NISHIMURA, AND J. UGANDER, *Configuring random graph models with fixed degree sequences*, SIAM Review, 60 (2018), pp. 315–355.
 - [26] X. FU, S. YU, AND A. R. BENSON, *Modeling and analysis of tagging networks in stock exchange communities*, Journal of Complex Networks, (2019), pp. 1–19.
 - [27] E. GODEHARDT AND J. JAWORSKI, *Two models of random intersection graphs for classification*, in Exploratory data analysis in empirical research, Springer, 2003, pp. 67–81.
 - [28] K.-I. GOH, M. E. CUSICK, D. VALLE, B. CHILDS, M. VIDAL, AND A.-L. BARABASI, *The human disease network*, Proceedings of the National Academy of Sciences, 104 (2007), pp. 8685–8690.
 - [29] M. S. GRANOVETTER, *The strength of weak ties*, in Social networks, Elsevier, 1977, pp. 347–367.
 - [30] R. GUIMERA, M. SALES-PARDO, AND L. A. N. AMARAL, *Module identification in bipartite and directed networks*, Physical Review E, 76 (2007).
 - [31] M. O. JACKSON AND B. W. ROGERS, *Meeting strangers and friends of friends: How random are social networks?*, American Economic Review, 97 (2007), pp. 890–915.
 - [32] B. KARRER AND M. E. J. NEWMAN, *Stochastic blockmodels and community structure in networks*, Physical Review E, 83 (2011).
 - [33] D. B. LARREMORE, A. CLAUSET, AND A. Z. JACOBS, *Efficiently inferring community structure in bipartite networks*, Physical Review E, 90 (2014).
 - [34] M. LATAPY, *Main-memory triangle computations for very large (sparse (power-law)) graphs*, Theor. Comput. Sci., 407 (2008), pp. 458–473.
 - [35] S. LATTANZI AND D. SIVAKUMAR, *Affiliation networks*, in Proceedings of the 41st annual ACM Symposium on Theory of Computing (STOC), 2009.
 - [36] J. LESKOVEC, L. A. ADAMIC, AND B. A. HUBERMAN, *The dynamics of viral marketing*, ACM Transactions on the Web (TWEB), 1 (2007), pp. 5–es.

- [37] P. LI AND O. MILENKOVIC, *Inhomogeneous hypergraph clustering with applications*, in Advances in Neural Information Processing Systems, 2017, pp. 2308–2318.
- [38] J. NACHER AND T. AKUTSU, *On the degree distribution of projected networks mapped from bipartite networks*, Physica A: Statistical Mechanics and its Applications, 390 (2011), pp. 4636–4651.
- [39] Z. NEAL, *The backbone of bipartite projections: Inferring relationships from co-authorship, co-sponsorship, co-attendance and other co-behaviors*, Social Networks, 39 (2014), pp. 84–97.
- [40] M. E. NEWMAN, *The structure of scientific collaboration networks*, Proceedings of the National Academy of Sciences, 98 (2001), pp. 404–409.
- [41] M. E. NEWMAN, *The structure and function of complex networks*, SIAM Review, 45 (2003), pp. 167–256.
- [42] M. E. J. NEWMAN, *Coauthorship networks and patterns of scientific collaboration*, Proceedings of the National Academy of Sciences, 101 (2004), pp. 5200–5205.
- [43] M. E. J. NEWMAN, S. H. STROGATZ, AND D. J. WATTS, *Random graphs with arbitrary degree distributions and their applications*, Phys. Rev. E, 64 (2001), p. 026118.
- [44] T. OPSAHL, *Triadic closure in two-mode networks: Redefining the global and local clustering coefficients*, Social Networks, 35 (2013), pp. 159–167.
- [45] M. A. PORTER, P. J. MUCHA, M. E. J. NEWMAN, AND C. M. WARMBRAND, *A network analysis of committees in the U.S. House of Representatives*, Proceedings of the National Academy of Sciences, 102 (2005), pp. 7057–7062.
- [46] A. RAPOPORT, *Spread of information through a population with socio-structural bias: I. assumption of transitivity*, The bulletin of mathematical biophysics, 15 (1953), pp. 523–533.
- [47] E. RAVASZ, A. L. SOMERA, D. A. MONGRU, Z. N. OLTVAI, AND A.-L. BARABÁSI, *Hierarchical organization of modularity in metabolic networks*, science, 297 (2002), pp. 1551–1555.
- [48] H. J. RYSER, *Combinatorial mathematics*, vol. 14, American Mathematical Soc., 1963.
- [49] C. SEIERSTAD AND T. OPSAHL, *For the few not the many? the effects of affirmative action on presence, prominence, and social capital of women directors in norway*, Scandinavian Journal of Management, 27 (2011), pp. 44–54.
- [50] C. SESHADHRI, T. G. KOLDA, AND A. PINAR, *Community structure and scale-free collections of Erdős-Rényi graphs*, Physical Review E, 85 (2012), p. 056109.
- [51] J. SUN, H. QU, D. CHAKRABARTI, AND C. FALOUTSOS, *Neighborhood formation and anomaly detection in bipartite graphs*, in Fifth IEEE International Conference on Data Mining, IEEE, 2005.
- [52] G. SZABÓ, M. ALAVA, AND J. KERTÉSZ, *Structural transitions in scale-free networks*, Physical Review E, 67 (2003), p. 056102.
- [53] A. TAUDIERE, F. MUNOZ, A. LESNE, A.-C. MONNET, J.-M. BELLANGER, M.-A. SELOSSE, P.-A. MOREAU, AND F. RICHARD, *Beyond ectomycorrhizal bipartite networks: projected networks demonstrate contrasted patterns between early- and late-successional plants in corsica*, Frontiers in Plant Science, 6 (2015).
- [54] C.-Y. TENG, Y.-R. LIN, AND L. A. ADAMIC, *Recipe recommendation using ingredient networks*, in Proceedings of the 3rd Annual ACM Web Science Conference, ACM Press, 2012.
- [55] N. VELDT, A. R. BENSON, AND J. KLEINBERG, *Localized flow-based clustering in hypergraphs*, in Proceedings of the SIGKDD Conference on Knowledge Discovery and Data Mining, 2020.
- [56] I. VOGT AND J. MESTRES, *Drug-target networks*, Molecular Informatics, 29 (2010), pp. 10–14.
- [57] D. J. WATTS AND S. H. STROGATZ, *Collective dynamics of ‘small-world’ networks*, Nature, 393 (1998), p. 440.
- [58] S. A. WILLIAMSON AND M. TEC, *Random clique covers for graphs with local density and global sparsity*, in Proceedings of the Conference on Uncertainty in Artificial Intelligence, 2019.
- [59] J. YANG AND J. LESKOVEC, *Community-affiliation graph model for overlapping network community detection*, in 2012 IEEE 12th International Conference on Data Mining, IEEE, Dec. 2012.
- [60] H. YIN, A. R. BENSON, AND J. LESKOVEC, *The local closure coefficient: a new perspective on network clustering*, in Proceedings of the Twelfth ACM International Conference on Web Search and Data Mining, ACM, 2019, pp. 303–311.
- [61] H. YIN, A. R. BENSON, AND J. UGANDER, *Measuring directed triadic closure with closure coefficients*, Network Science, (2020), pp. 1–23.
- [62] Y. ZHANG, A. FRIEND, A. L. TRAUD, M. A. PORTER, J. H. FOWLER, AND P. J. MUCHA, *Community structure in congressional cosponsorship networks*, Physica A: Statistical Mechanics and its Applica-

tions, 387 (2008), pp. 1705–1712.

- [63] D. ZHOU, J. HUANG, AND B. SCHÖLKOPF, *Learning with hypergraphs: Clustering, classification, and embedding*, in Advances in neural information processing systems, 2007, pp. 1601–1608.
- [64] T. ZHOU, J. REN, M. C. V. MEDO, AND Y.-C. ZHANG, *Bipartite network projection and personal recommendation*, Phys. Rev. E, 76 (2007), p. 046115.

Appendix A. Connection between conditional probability and empirical clustering.

Here, we show that the conditional probability formulation for clustering is exactly a weighted average of the standard empirical clustering coefficient for the power-law type distributions our model explores. We demonstrate this below for the local clustering coefficient. The case for local closure is similar.

Fix a node u and suppose we generate a graph G_i under our random graph model. Let W_i and T_i be the number of wedges and triangles at node u in the projected graph G_i . The empirical clustering coefficient $\tilde{C}_i(u)$ is equal to T_i/W_i . Weighting each sample \tilde{C}_i by W_i , the weighted clustering coefficient is $\frac{\sum_{i=1}^s W_i \tilde{C}_i(u)}{\sum_{i=1}^s W_i} = \frac{\frac{1}{s} \sum_{i=1}^s T_i}{\frac{1}{s} \sum_{i=1}^s W_i}$. As the number of samples s (i.e. the size of the graph) approaches infinity, both the numerator and denominator approaches their expectations since each sample is independent. Computing this expectation, we see that it is exactly the value of $C(u)$ computed in Theorem 3.8.

In the case of the global closure coefficient, a similar argument shows that we actually have equality between the conditional and non-conditional definition (in the limit that the size of the graph goes to infinity).

Appendix B. Power-law statistics in real-world bipartite networks. In many of our datasets, we find that power-law degree distributions are a reasonable approximation for the left and right sides of the bipartite network (Table B.1).

Table B.1: Estimated power law (PL) exponents of the left and right degree distributions in the bipartite graph datasets in Table 5.2 (an exponent of α corresponds to a distribution decay $\propto k^{-\alpha}$). Parameters were fit using the `powerlaw` python package [4]. We also report the Kolmogorov-Smirnov statistic D between the fit model and the data.

dataset	left PL exponent	D	right PL exponent	D
actors-movies	1.862 ± 0.002	0.025	5.066 ± 0.080	0.019
amazon-products-pages	3.426 ± 0.028	0.009	1.530 ± 0.001	0.310
classes-drugs	2.179 ± 0.088	0.055	2.528 ± 0.007	0.060
condmat-authors-papers	3.495 ± 0.085	0.039	7.739 ± 0.829	0.017
directors-boards	4.799 ± 0.400	0.055	5.390 ± 1.007	0.085
diseases-genes	3.105 ± 0.190	0.043	3.120 ± 0.138	0.053
genes-diseases	3.120 ± 0.138	0.053	3.105 ± 0.190	0.043
mathsx-tags-questions	1.835 ± 0.048	0.048	5.909 ± 0.015	0.012
mo-questions-users	2.842 ± 0.061	0.017	1.642 ± 0.008	0.031
so-users-threads	2.407 ± 0.009	0.011	7.263 ± 0.149	0.015
walmart-items-trips	2.586 ± 0.039	0.014	2.217 ± 0.005	0.108

Appendix C. Additional proofs.

Proof of Lemma 3.9. Let A_i denote the event that $(u, u_i) \in E$ for $i = 1, 2$. We want to compute the probability of $A_1 \cap A_2$. We first decompose the probability as follows:

$$(C.1) \quad \mathbb{P}[A_1 \cap A_2] = \mathbb{P}[A_1] + \mathbb{P}[A_2] - \mathbb{P}[A_1 \cup A_2] = \mathbb{P}[A_1] + \mathbb{P}[A_2] + \mathbb{P}[\bar{A}_1 \cap \bar{A}_2] - 1.$$

The probability that events A_i occur is given by Theorem 3.4, so we compute the probability of $\bar{A}_1 \cap \bar{A}_2$, which is the event that u is not connected to either u_1 or u_2 in the projected graph. This happens if and only if, in the bipartite graph, for every $v \in R$, we have that (i) u is not connected to v , or (ii) both u_1 and u_2 are not connected to v . For now, let v be a fixed node on the right. Conditioning on w_v and using the fact that edge formations in the bipartite graph are independent, the probability is

$$1 - \frac{w_u w_v}{n_R M_{R1}} + \frac{w_u w_v}{n_R M_{R1}} \left(1 - \frac{w_{u_1} w_v}{n_R M_{R1}}\right) \left(1 - \frac{w_{u_2} w_v}{n_R M_{R1}}\right) = 1 - \frac{w_u (w_{u_1} + w_{u_2}) w_v^2}{n_R^2 M_{R1}^2} + \frac{w_u w_{u_1} w_{u_2} w_v^3}{n_R^3 M_{R1}^3}.$$

Therefore, we have

$$\begin{aligned} \log(\mathbb{P}[\bar{A}_1 \cap \bar{A}_2]) &= \sum_{v \in R} \log \left(1 - \frac{w_u (w_{u_1} + w_{u_2}) w_v^2}{n_R^2 M_{R1}^2} + \frac{w_u w_{u_1} w_{u_2} w_v^3}{n_R^3 M_{R1}^3}\right) \\ &= \sum_{v \in R} \left[-\frac{w_u (w_{u_1} + w_{u_2}) w_v^2}{n_R^2 M_{R1}^2} + \frac{w_u w_{u_1} w_{u_2} w_v^3}{n_R^3 M_{R1}^3} - \frac{w_u^2 (w_{u_1} + w_{u_2})^2 w_v^4}{2n_R^4 M_{R1}^4} \cdot (1 + O(n_R^{-2\delta})) \right] \\ &= -p_{uu_1} - p_{uu_2} + \frac{M_{R1} M_{R3}}{M_{R2}^2} p_{uu_1} p_{uu_2} \frac{1}{w_u} - \frac{M_{R4}}{2n_R M_{R2}^2} (p_{uu_1} + p_{uu_2})^2 \cdot (1 + O(n_R^{-2\delta})). \end{aligned}$$

Consequently,

$$\begin{aligned} \mathbb{P}[\bar{A}_1 \cap \bar{A}_2] &= 1 - p_{uu_1} - p_{uu_2} + \frac{p_{uu_1}^2}{2} + \frac{p_{uu_2}^2}{2} + p_{uu_1} p_{uu_2} - \frac{p_{uu_1}^3 + p_{uu_2}^3}{6} (1 + O(n_R^{-2\delta})) + o(p_{uu_1} p_{uu_2}) \\ &\quad + \frac{M_{R1} M_{R3}}{M_{R2}^2} p_{uu_1} p_{uu_2} \frac{1}{w_u} \cdot (1 + O(n_R^{-2\delta})) - \frac{M_{R4}}{2n_R M_{R2}^2} (p_{uu_1}^2 + p_{uu_2}^2) (1 + O(n_R^{-2\delta})). \end{aligned}$$

Combining everything, the probability of wedge formation is

$$\begin{aligned} \mathbb{P}[A_1 \cap A_2] &= \left(\frac{M_{R1} M_{R3}}{M_{R2}^2} \cdot \frac{1}{w_u} + 1 \right) p_{uu_1} p_{uu_2} \cdot (1 + O(n_R^{-2\delta}) + o(1)) \\ &\quad + \left(\frac{p_{uu_1} + p_{uu_2}}{6} + \frac{M_{R4}}{2n_R M_{R2}^2} \right) (p_{uu_1}^2 + p_{uu_2}^2) \cdot O(n_R^{-2\delta}) \\ &= \left(\frac{M_{R1} M_{R3}}{M_{R2}^2} \cdot \frac{1}{w_u} + 1 \right) p_{uu_1} p_{uu_2} \cdot \left(1 + O(n_R^{-2\delta}) + o(1) + \left(\frac{w_{u_1}}{w_{u_2}} + \frac{w_{u_2}}{w_{u_1}} \right) O(n_R^{-4\delta}) \right) \\ &= \left(\frac{M_{R1} M_{R3}}{M_{R2}^2} \cdot \frac{1}{w_u} + 1 \right) p_{uu_1} p_{uu_2} \cdot \left(1 + O(n_R^{-2\delta}) + o(1) + O(n_R^{1/2-5\delta}) \right) \end{aligned}$$

where the last equality is due to $w_{u_i} \in [1, n^{1/2-\delta}]$ and their ratio is bounded by $n^{1/2-\delta}$. Since $\delta > 1/10$, the proof is complete.

Proof of Lemma 3.10. For nodes u, u_1, u_2 to form a triangle, one of two cases must happen. The first is the case that all three nodes connect to a same node in the right partition. If the first case does not happen, then each pair (u, u_1) , (u, u_2) , (u_1, u_2) have a different common neighbor in the bipartite graph, forming a length-6 cycles. Now we analyze these two cases separately.

In the first case, there exists a node $v \in R$ such that the three nodes u, u_1, u_2 are connected to v . For any specific node $v \in R$, the probability is $\frac{w_u w_{u_1} w_{u_2}}{n_R^3 M_{R1}^3} \cdot w_v^3$, and thus

$$\begin{aligned} \mathbb{P}[\exists v \in R \text{ s.t. } (u, v), (u_1, v), (u_2, v) \in E_b] &= 1 - \prod_{v \in R} \left(1 - \frac{w_u w_{u_1} w_{u_2}}{n_R^3 M_{R1}^3} \cdot w_v^3\right) \\ &= 1 - \exp\left(-\frac{w_u w_{u_1} w_{u_2}}{n_R^3 M_{R1}^3} \cdot \sum_{v \in R} w_v^3 \cdot (1 + O(n_R^{-6\delta}))\right) = p_{uu_1} p_{uu_2} \cdot \frac{M_{R1} M_{R3}}{M_{R2}^2} \cdot \frac{1}{w_u} \cdot (1 + O(n_R^{-3\delta})). \end{aligned}$$

In the second case, u, u_1, u_2 are pairwise connected through a different node on the right separately, forming a 6-cycle. For any node triple v_1, v_2, v_3 , the probability is

$$\mathbb{P}[(u, v_1, u_1, v_2, u_2, v_3) \text{ forms a 6-cycle}] = \frac{w_u^2 w_{u_1}^2 w_{u_2}^2}{n_R^6 M_{R1}^6} \cdot w_{v_1}^2 w_{v_2}^2 w_{v_3}^2.$$

Therefore, the total probability of the second case is

$$\begin{aligned} \mathbb{P}[\exists \text{ a 6-cycle containing } u, u_1, u_2] &\leq \sum_{\substack{v_1, v_2, v_3 \in R \\ v_1 \neq v_2 \neq v_3}} \frac{w_u^2 w_{u_1}^2 w_{u_2}^2}{n_R^6 M_{R1}^6} \cdot w_{v_1}^2 w_{v_2}^2 w_{v_3}^2 \\ &\leq \frac{w_u^2 w_{u_1}^2 w_{u_2}^2}{n_R^3 M_{R1}^6} \cdot \frac{\sum_{v_1 \in R} w_{v_1}^2}{n_R} \frac{\sum_{v_2 \in R} w_{v_2}^2}{n_R} \frac{\sum_{v_3 \in R} w_{v_3}^2}{n_R} = p_{uu_1} p_{uu_2} p_{u_1 u_2} = o(p_{uu_1} p_{uu_2}). \end{aligned}$$

Combining the two cases completes the proof.